Dyes and Pigments xxx (xxxx) xxx

Contents lists available at ScienceDirect

Dyes and Pigments

journal homepage: http://www.elsevier.com/locate/dyepig

Planar and sandwich-type Pr(III) and Nd(III) chlorinated phthalocyaninates: Synthesis, thermal stability and optical properties

Elena A. Kuzmina [a,b], Tatiana V. Dubinina [a,b,*], Nataliya E. Borisova [a,c], Boris N. Tarasevich [a], Vitaly I. Krasovskii [d], Ivan N. Feofanov [d], Alexander V. Dzuban [a], Larisa G. Tomilova [a,b]

[a] Department of Chemistry, Lomonosov Moscow State University, 1 Leninskie Gory, 119991, Moscow, Russian Federation
[b] Institute of Physiologically Active Compounds, Russian Academy of Sciences, 1 Severny Proezd, 142432, Chernogolovka, Moscow Region, Russian Federation
[c] A.N. Nesmeyanov Institute of Organoelement Compounds, 28 Vavilov Str, 119334, Moscow, Russian Federation
[d] Prokhorov General Physics Institute, Russian Academy of Sciences, 119991, 38, Vavilov Street, Moscow, Russian Federation

ARTICLE INFO

Keywords:
Phthalocyanines
Double-decker complex
Stabilized redox state
Lanthanides
Nonlinear optical properties
Thermogravimetry

ABSTRACT

A direct synthetic approach to four single-decker and one double-decker novel Pr(III) and Nd(III) complexes with 2,3,9,10,16,17,23,24-octachlorophthalocyaninate and 1,2,3,4,8,9,10,11,15,16,17,18,22,23,24,25-hexadeca-chlorophthalocyaninate has been developed. Synthesis of hexadeca-Cl-substituted Nd(III) *bis*phthalocyaninate has been carried out utilizing two preformed synthetic blocks: Nd(III) octachlorophthalocyaninate acetate and octachlorophthalocyanine ligand. Due to the electron withdrawing effect of 16 chlorine groups, this Nd(III) *bis*phthalocyaninate was obtained as a redox stable anionic form. Upfield lanthanide-induced shifts of the aromatic proton signals (up to 2.04 ppm for Pr(III) octachlorophthalocyaninate acetate) were observed in the ^{1}H NMR spectra of the obtained phthalocyaninates. Thermal stability of the lanthanide (III) complexes was examined using thermogravimetric analysis combined with mass-spectrometry. The double-decker compound was shown to possess an increased thermal stability in comparison with the single-deckers up to ~400 °C. Linear and nonlinear optical properties of the Cl-substituted Nd(III) and Pr(III) phthalocyaninates have been investigated using z-scan technique. The best nonlinear optical response with the highest excited state absorption cross-section ($\sigma_1 = 1.1 \times 10^{-15}$ cm^{-2}) was found for the hexadeca-Cl-substituted Nd(III) *mono*phthalocyaninate.

1. Introduction

Introduction of electron-withdrawing groups in the phthalocyanine macrocycle results in appearance of n-type conductivity [1–3], enchanced oxidation stability in comparison with unsubstituted analogs [4,5]. In particular, it was shown [4] that introduction of N-substituted phthalimide groups in the sandwich-type lanthanide (III) *bis*phthalocyaninates leads to a strong anodic shift of approximately 0.7 V of their first oxidation potentials comparing to the corresponding unsubstituted lanthanide (III) *bis*phthalocyaninates.

Nonlinear optics is one of the most promising application areas of phthalocyanines and their analogs [6–8]. Nonlinear optical materials can be employed to control optical signals, which is widely used in photovoltaic, optical communication and imaging, photodynamic therapy and surgery [9]. The presence of nonlinear optical response allows using of phthalocyanines and materials based on them as optical limiters – materials, which are characterized by a decrease in optical transmittance under the strong illumination [8,10,11]. Phthalocyanines bearing electron-withdrawing functional groups exhibit enchanced optical limiting response comparing to the unsubstituted congeners. It was demonstrated that the presence of fluoro-groups [12] in the phthalocyanine brings about a noticeable improvement of the optical limiting effect. Due to a strong aggregation tendency, phthalocyanines bearing electron-withdrawing groups possess low solubility in common organic solvents. Thus, the development of synthetic approaches to novel well-soluble phthalocyanines with electron-deficient moieties is an important problem. It can be solved by obtaining lanthanide (III) phthalocyaninates. The presence of both a bulky central ion (Ln^{3+}) and an axial extra ligand suppresses aggregation. Additionally, it is well known [6] that the presence of a heavy atom can improve nonlinear optical response of target compounds due to enhanced triplet state absorption [13]. Thus, the most prospective central ions are the lanthanides of the beginning of the row (namely, Pr and Nd) with large ionic radii.

* Corresponding author. Department of Chemistry, Lomonosov Moscow State University, 1 Leninskie Gory, 119991, Moscow, Russian Federation.
E-mail address: dubinina.t.vid@gmail.com (T.V. Dubinina).

https://doi.org/10.1016/j.dyepig.2019.108075
Received 24 August 2019; Received in revised form 23 November 2019; Accepted 25 November 2019
Available online 26 November 2019
0143-7208/

Double-decker phthalocyanine complexes, bearing electron-withdrawing functional groups may be advantageous due to their stability to oxidation [11]. Moreover, the introduction of electron-withdrawing substituents to the double-decker molecules leads to an increase in the effective energy barrier and improvement of SMM properties [14]. However, only little attention has been paid to halogen substituted Ln (III) *bis*phthalocyaninates [15].

The present study is devoted to the development of selective and effective synthetic approaches and investigation of optical (linear and nonlinear) properties of novel single-decker and double-decker Pr(III) and Nd(III) chlorinated phthalocyaninates.

2. Experimental

2.1. Chemicals and instruments

All the reactions were monitored by thin-layer chromatography (TLC) and UV–Vis spectra until the complete disappearance of the starting reagents was observed unless otherwise specified. TLC was performed using Merck Aluminium Oxide F_{254} neutral flexible plates. Gel permeation chromatography was accomplished on polymeric support Bio-Beads S-X1 (BIORAD).

Electronic absorption (UV–Vis) spectra were recorded on a JASCO V-770 spectrophotometer using quartz cells (1 × 1 cm). Matrix assisted laser desorption/ionization time-of-flight (MALDI TOF) mass spectra were taken on a Bruker Autoflex II mass spectrometer with α-cyano-4-hydroxycinnamic acid (CHCA) as the matrix. High-resolution MALDI mass spectra were registered on a Bruker ULTRAFLEX II TOF/TOF instrument with α-cyano-4-hydroxycinnamic acid (CHCA) as the matrix. The salts $Pr(OAc)_3 \times H_2O$ and $Nd(OAc)_3 \times H_2O$ were dried at 70 °C for 3 h immediately before use. 4,5-Dichlorophthalonitrile (Sigma–Aldrich) and tetrachlorophthalonitrile (Sigma–Aldrich) were used as received. 2,3,9,10,16,17,23,24-Octachlorophthalocyanine **2a** and 1,2,3,4,8,9,10,11,15,16,17,18,22,23,24,25-hexadecachlorophthalocyanine **2b** were obtained according to the previously described method [16].

IR spectral measurements were carried out using Thermo Scientific Nicolet iS5 FT-IR spectrometer in KBr or on the working surface of the internal reflection (ATR) diamond element. Spectral resolution: $\Delta\lambda = 4$ cm^{-1}.

^1H NMR spectra were recorded on a Bruker AVANCE 600 spectrometer (600.13 MHz). Chemical shifts are given in ppm relative to $SiMe_4$.

Thermal analysis (TG-DTA-MS) was carried out by using STA 409 PC Luxx (NETZSCH) simultaneous thermal analyzer coupled with QMS 403C Aëolos quadrupole mass spectrometer. Measurements were performed in alumina crucibles (V = 0.9 ml) up to 1000 °C with a heating rate of 10 °C·min^{-1} under inert (Ar) atmosphere.

The measurement of nonlinear optical properties was carried out using a well known Z-scan technique [17]. Second harmonic of a Q-switched YAG:Nd laser (0.53 μm wavelength, 20 ns pulse duration, 5 Hz repetition rate) was used for the excitation. Average single pulse energy measured with Ophir Pulsar 2 energy meter was 250 μJ. Laser radiation was focused using a 10 cm focal length lens.

2.2. Synthesis and identification

2.2.1. Preparation of 2,3,9,10,16,17,23,24-octachlorophthalocyaninato praseodymium acetate *3a*

A mixture of 2,3,9,10,16,17,23,24-octachlorophthalocyanine **2a** (157.0 mg, 0.2 mmol) and $Pr(OAc)_3 \times H_2O$ (64.0 mg, 0.2 mmol) was refluxed in 2.5 mL of 1,2-dichlorobenzene in the presence of 1,8-diazabicyclo [5.4.0]undec-7-ene (72 μL, 0.48 mmol) for 4 h (TLC–control: SiO_2, F_{254}, toluene). The reaction mixture was cooled to room temperature and a MeOH:H_2O (4:1 V/V) mixture was added. The precipitate was filtered and washed with a MeOH:H_2O (4:1 V/V) mixture and dried at 70 °C to give compound **3a** (147.0 mg, 75%). UV–Vis (THF): λ_{max} (nm) 346 (lgε 4.57); 672 (4.89). IR (diamond): ν (cm^{-1}) 1045–1068 (st C–Cl); 1535 (γ-pyrrole); 1388–1404 (st COO^- sym); 1535–1627 (st COO^- asym); 2852–2939 (st CH from OAc). MS (MALDI-TOF): *m/z* 925 [M − OAc, 100%], 984 [M, 40%]. MS (MALDI-TOF/TOF): *m/z* Found: 983.7557 [M]; molecular formula $C_{34}H_{11}Cl_8N_8O_2Pr$ requires 983.7590 [M]. ^1H NMR (THF-d_8, 293 K) δ_H ppm: 2.04 (s, H_{Pc}).

2.2.2. Preparation of 1,2,3,4,8,9,10,11,15,16,17,18,22,23,24,25-hexadecachlorophthalocyaninato praseodymium acetate *3b*

A mixture of 1,2,3,4,8,9,10,11,15,16,17,18,22,23,24,25-hexadecachlorophthalocyanine **2b** (100.0 mg, 0.09 mmol) and $Pr(OAc)_3 \times H_2O$ (30.0 mg, 0.09 mmol) was refluxed in 2.5 mL of 1,2-dichlorobenzene (*o*-DCB) in the presence of 1,8-diazabicyclo [5.4.0]undec-7-ene (35 μL, 0.23 mmol) for 4 h (TLC–control: SiO_2, F_{254}, toluene). The reaction mixture was cooled to room temperature and a MeOH:H_2O (4:1 V/V) mixture was added. The precipitate was filtered and washed with a MeOH:H_2O (4:1 V/V) mixture and dried at 70 °C to give compound **3b** (75.0 mg, 68%). UV–Vis (THF): λ_{max} (nm) 379 (lgε 3.99); 693 (4.52). IR (diamond): ν (cm^{-1}) 1037–1121 (st C–Cl); 1522–1539 (γ-pyrrole); 1370–1435 (st COO^- sym); 1522–1539 (st COO^- asym); 2835–2920 (st CH from OAc). MS (MALDI-TOF): *m/z* 1163 [M-OAc-Cl, 20%]; 1197 [M − OAc, 47%]; 1256 [M + H, 100%]; 1315 [M-OAc-Cl + DBU, 84%]; 1367 [M-OAc + OH + DBU, 33%]. MS (MALDI-TOF/TOF): *m/z* Found: 1256.4352 [M+H]; molecular formula $C_{34}H_4Cl_{16}N_8O_2Pr$ requires 1256.4550 [M+H].

2.2.3. Preparation of 2,3,9,10,16,17,23,24-octachlorophthalocyaninato neodymium acetate *4a*

A mixture of 2,3,9,10,16,17,23,24-octachlorophthalocyanine **2a** (75.0 mg, 0.1 mmol) and $Nd(OAc)_3 \times H_2O$ (32.2 mg, 0.1 mmol) was refluxed in 2 mL of 1,2-dichlorobenzene in the presence of 1,8-diazabicyclo [5.4.0]undec-7-ene (23 μL, 0.16 mmol) for 4 h (TLC–control: SiO_2, F_{254}, toluene). The reaction mixture was cooled to room temperature and a MeOH:H_2O (4:1 V/V) mixture was added. The precipitate was filtered and washed with a MeOH:H_2O (4:1 V/V) mixture and dried at 70 °C to give compound **4a** (72.0 mg, 73%). UV–Vis (THF): λ_{max} (nm) 349 (lgε 4.74); 673 (4.42). IR (KBr): ν (cm^{-1}) 1010–1080 (st C–Cl); 1504 (γ-pyrrole); 1375–1421 (st COO^- sym); 1504 (st COO^- asym); 2933–3087 (st CH from OAc). MS (MALDI-TOF): *m/z* 925 [M − OAc, 100%]; 985 [M, 60%]. MS (MALDI-TOF/TOF): *m/z* Found: 984.7347 [M]; molecular formula $C_{34}H_{11}Cl_8N_8NdO_2$ requires 984.7590 [M]. ^1H NMR (THF-d_8, 293 K) δ_H ppm: 4.74 (s, H_{Pc}).

2.2.4. Preparation of 1,2,3,4,8,9,10,11,15,16,17,18,22,23,24,25-hexadecachlorophthalocyaninato neodymium acetate *4b*

A mixture of 1,2,3,4,8,9,10,11,15,16,17,18,22,23,24,25-hexadecachlorophthalocyanine **2b** (55.0 mg, 0.05 mmol) and $Nd(OAc)_3 \times H_2O$ (17.0 mg, 0.05 mmol) was refluxed in 1.5 mL of 1,2-dichlorobenzene in the presence of 1,8-diazabicyclo [5.4.0]undec-7-ene (18 μL, 0.12 mmol) for 4 h (TLC–control: SiO_2, F_{254}, toluene). The reaction mixture was cooled to room temperature and a MeOH:H_2O (4:1 V/V) mixture was added. The precipitate was filtered and washed with a MeOH:H_2O (4:1 V/V) mixture and dried at 70 °C to give compound **4b** (50.0 mg, 76%). UV–Vis (THF): λ_{max} (nm) 378 (lgε 4.57); 694 (5.02). IR (KBr): ν (cm^{-1}) 1097–1136 (st C–Cl); 1508–1541 (γ-pyrrole); 1327–1421 (st COO^- sym); 1508–1639 (st COO^- asym); 2868–2954 (st CH from OAc). MS (MALDI-TOF, negative mode): *m/z* 1408 [M + DBU, 20%]; 1578 [M+2DBU + H_2O, 68%]; 1634 [M+2CHCA, 100%]; 1693 [M+2CHCA + OAc, 82%]; 1730 [M+3DBU + H_2O, 82%]. MS (MALDI-TOF/TOF): *m/z* Found: 1408.5842 [M + DBU]; molecular formula $C_{43}H_{19}Cl_{16}N_{10}NdO_2$ requires 1408.5786 [M + DBU].

*2.2.5. Preparation of bis[2,3,9,10,16,17,23,24-octachlorophthalocyaninato] neodymium **5***

2.2.5.1. Method A. 4,5-Dichlorophthalonitrile (158.0 mg, 0.6 mmol), $Nd(OAc)_3 \times H_2O$ (67.8 mg, 0.2 mmol) and 1,8-diazabicyclo [5.4.0] undec-7-ene (119 μL, 0.8 mmol) were stirred in 3 mL of boiling iso-amil alcohol for 4 h (TLC-control: SiO_2, F_{254}, toluene). The reaction mixture was cooled to room temperature and a MeOH:H_2O (4:1 V/V) mixture was added. The precipitate was filtered and washed with a MeOH: H_2O (4:1 V/V) mixture and dried at 70°C. Gel permeation chromatography (THF) was employed to isolate *bis*phthalocyanine complex. After the solvent was evaporated from the collected fraction of target compound, the residue was washed with MeOH and dried at room temperature to give complex **5** (13.0 mg, 10%). UV–Vis (THF): λ_{max} (nm) 340 (lgε 4.69); 637 (4.57) and 682 (4.41). MS (MALDI-TOF, negative mode): *m/z* 1719 [M − H]$^-$. MS (MALDI-TOF/TOF): *m/z* Found: 1719.3987 [M − H, 100%]$^-$; molecular formula $C_{64}H_{15}Cl_{16}N_{16}Nd$: 1719.3991 [M − H, 100%]$^-$. ^{1}H NMR (THF-d_8, 293 K) δ_H ppm: 5.88 (s, H_{Pc}).

2.2.5.2. Method B. A mixture of 2,3,9,10,16,17,23,24-octachlorophthalocyanine **2** (33.0 mg, 0.04 mmol), complex **4a** (40.0 mg, 0.04 mmol), and $C_{16}H_{33}OH$ (14 mg) and catalytic amount of lithium methoxide were heated at 220 °C in 2 mL of 1,2,4-trichlorobenzene for 2 h. The reaction mixture was cooled to room temperature and a MeOH:H_2O (4:1 V/V) mixture was added. The precipitate was filtered and washed with a MeOH:H_2O (4:1 V/V) mixture and dried at 70 °C to give compound **5** (60.0 mg, 87%). The characteristics were identical with those obtained by method (A).

3. Results and discussion

3.1. Synthesis and identification

Lanthanide (III) phthalocyaninates can be obtained using two approaches: template synthesis and multi-step approach through the assembly of phthalocyanine ligand [16,18,19]. It was earlier demonstrated [16,20], that the second way is more preferable for lanthanide (III) phthalocyaninates with large ionic radius of central ion. This is probably results from the steric reasons.

According to the method based on phthalocyanine ligands, magnesium complexes **1a** and **1b** were obtained using earlier described procedure [16]. Then they were demetallated by saturated sulfuric acid to give corresponding chloro-substituted phthalocyanines **2a** and **2b**. The last stage was performed in boiling 1,2-dichlorobenzene (*o*-DCB) in a presence of 1,8-diazabicyclo [5.4.0]undec-7-ene (DBU) as a base (Scheme 1).

In the case of halogen-substituted phthalocyanine complexes, the employment of commonly used alkali metal alkoxides as base reagents is not suitable due to the possibility of nucleophilic substitution typical for the electron-deficient systems [21]. In the case of DBU, no traces of the nucleophilic substitution products were observed.

Noteworthy, that increase in ionic radius of central lanthanide ion from Lu^{3+} to Nd^{3+} and Pr^{3+} lead to increase the quantity of sandwich-type by-products. In order to avoid the formation of sandwich-type complexes we use an excess of lanthanide acetate. Additionally, the DBU can provide the selectivity of formation of single-decker phthalocyanine complexes due to its coordination to the lanthanide central ion and appearance of steric hindrance [22].

The employment of present multi-step approach (Scheme 1) results in selective formation of single-decker Pr(III) and Nd(III) phthalocyaninates **3** and **4** respectively. The absence of sandwich-type byproducts was monitored by thin layer chromatography (TLC), UV–Vis spectroscopy and mass-spectrometry.

Our attempt to obtain chloro-substituted single-decker Nd(III) phthalocyaninate **3a** using the fast template approach was unsuccessful. In spite of presence of DBU and excess of lanthanide acetate the formation of mixture of mono- and *bis*phthalocyanine complexes was observed (Scheme 2). As it was earlier observed for phthalimide-substituted lanthanide (III) *bis*phthalocyaninates [4], double-decker complexes bearing electron-withdrawing functional groups, are stable anionic forms. Presence of electron-withdrawing functional groups in the periphery of phthalocyanine macrocycle results in stabilization of negative charge of the anionic state of the phthalocyanine complexes. *Bis*phthalocyanine complex **5**, which was separated from the reaction mixture, using gel permeation chromatography, is anionic form. It was proven using UV–Vis spectroscopy and mass-spectrometry in the negative ion mode.

Direct synthesis of neodymium (III) *bis*phthalocyaninate was carried out using two preformed synthetic blocks: phthalocyanine ligand **2a** and lanthanide (III) monophthalocyanine complex **4a**. The reaction was carried out in 1,2,4-trichlorobenzene (TCB) in a presence of cetyl alcohol ($C_{16}H_{33}OH$) and catalytic amount of lithium methoxide. The introduction of a larger amount of lithium methoxide results in the formation of a mixture of target compound **4a** and phthalocyanine complexes, containing different quantity of peripheral methoxy-groups due to nucleophilic substitution (mass spectrometry control). It can be explained by stronger basic nature of lithium methoxide in comparison with DBU.

Presence of cetyl alcohol allows increasing the boiling point of reaction mixture. In addition, cetyl alcohol is a source of alcohol ions, initiating the predominant formation of a sandwich complex [23–25]. Target complex **5** was obtained in a high yield (87%).

Target single- and double-decker complexes were identified by matrix assisted laser desorption/ionization time-of-flight (MALDI TOF) mass spectrometry (Fig. 1, Figs. S1–S3). The elemental composition of target complexes was proven using high resolution MALDI TOF/TOF mass spectrometry. The high resolution mass spectra demonstrated good agreement between the observed and calculated mass patterns (see Experimental part).

In the case of monophthalocyanine complexes **3a**, **3b** and **4a** corresponding molecular ions were observed. The isotopic distribution of the molecular ion peak is almost equal to theoretically calculated one. The

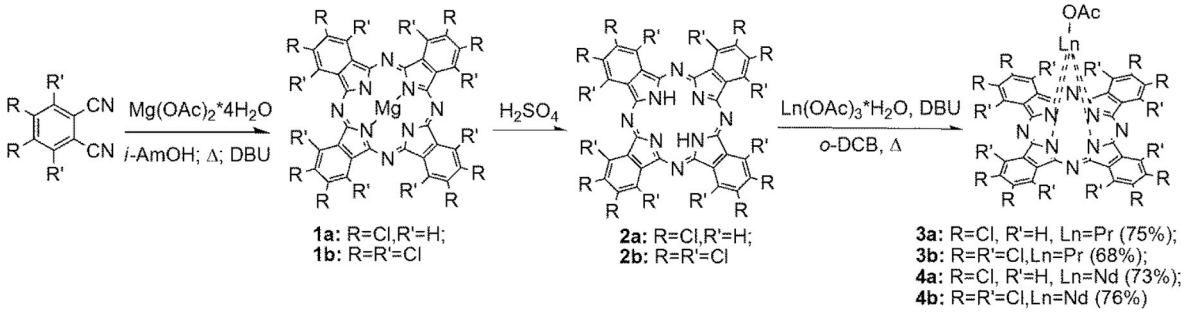

Scheme 1. Synthesis of octachloro- and hexadecachloro-substituted complexes.

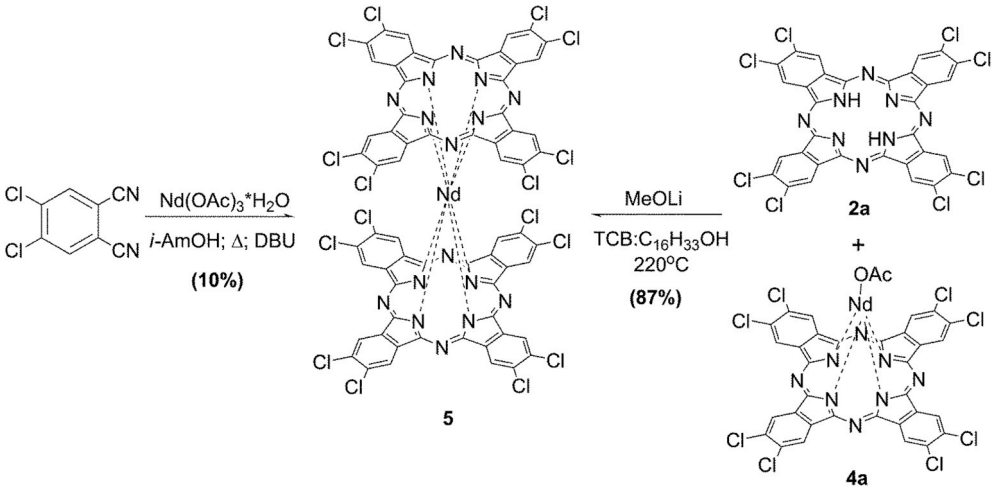

Scheme 2. Synthesis of *bis*phthalocyanine complex **5**.

additional fragmentation of axial acetate groups was found. Under laser ionization, the formation of adduct with CHCA matrix was detected in the case of monophthalocyanine complex **4b**. In the case of praseodymium complex **3b** and neodymium complex **4b** presence of coordinated molecule DBU was demonstrated. It can be explained by high coordination ability of the lanthanide ions.

Due to the anionic nature of neodymium (III) *bis*phthalocyaninate **5** mass spectrometry data for the positive ion mode were insufficient quality. Thus, the mass spectrum in the negative ion mode was measured for complex **5**. This complex shows only the peak corresponding to molecular ion [M − H] (Fig. 1).

In order to prove the presence of acetate anion as an axial ligand in target lanthanide monophthalocyaninates **3** and **4**, IR spectra were measured. In IR spectrum of complexes **3** and **4** stretching vibrations of C–Cl bonds were observed in the region of 1010–1136 cm^{-1} (Fig. 2, Figs. S4–S6). Skeletal vibrations of pyrrole moieties occupy the region from 1504 to 1541 cm^{-1}. Bands at 1504–1639 cm^{-1} and at 1327–1435 cm^{-1} were assigned to COO^- carboxylate ion asymmetric and symmetric stretching vibrations respectively. The presence of asymmetric and symmetric stretching vibrations of COO^- carboxylate ion results from the bidentate nature of OAc ligand.

Noteworthy, that the same values were observed for acetates in literature [26] and substituted lanthanide (III) monophthalocyaninates and monoporphyrazinates acetates reported by us earlier [16,18,20,27]. Stretching vibrations of CH from the axial acetate can be seen at 2835-3087 cm^{-1}.

In order to reach a better signal resolution in the ^1H NMR spectra of phthalocyanines **3a**, **4a** and **5** a polar coordinating solvent, namely, THF-d_8 was used. The presence of Pr(III) or Nd(III) central ions results in an upfield shift of the aromatic proton signals in the ^1H NMR spectra of **3a**, **4a** and **5** comparing to the corresponding octachloro-substituted diamagnetic Lu(III) phthalocyaninates [28] (Table 1).

The strongest upfield shift of the aromatic proton signals (2.04 ppm) was observed for praseodymium complex **3a**. In the case of single- and double-decker neodymium phthalocyaninates the chemical shifts correlate well with chemical shifts for aromatic protons of crown-substituted neodymium phthalocyaninates, described in literature [28].

Sandwich double-decker phthalocyanine complexes are usually obtained as the neutral forms of general formula $[Pc^{2-}Ln^{3+}Pc^{-}\cdot]^0$, which contain an unpaired π-electron. Therefore, their NMR spectra are generally measured for air-stable one-electron reduced anionic forms $[Ln^{3+}(Pc^{2-})_2]^-$ [5,23,24,30]. In order to obtain an anionic form of the double-decker complex, different reducing agents (N_2H_4, DBU, Na) are employed. However, in the case of compound **5**, the presence of electron-withdrawing groups leads to stabilization of the anionic form. Thus, its ^1H NMR spectrum was measured without any reducing agents. Small downfield shift of the aromatic proton signals was observed going from single-to double-decker neodymium complex. It results from deshielding effect of the second phthalocyanine macrocycle.

3.2. Thermal analysis

Thermogravimetry (Fig. 3A) revealed greater thermal stability of perchloro-substituted Pr(III) phthalocyaninate **3b** and double-decker complex **5** in comparison with octachloro-substitued Pr(III) phthalocyaninate (**3a**). Mass-spectra of evolved gases (Fig. 3B) show that decomposition of the latter one starts from water removal at 100 °C followed by elimination of acyl group at 300–390 °C (Fig. S9). Chlorine leaves gradually above 300 °C along with carbon-containing fragments during continuous destruction of complex.

For **3b** (Fig. 3C) all this processes begin almost simultaneously only when heated up to 300 °C. *Bis*phthalocyanine complex **5** (Fig. 3D) demonstrates slight mass change to 300 °C, which could be attributed to the loss of DBU remains. Thus, double-decker structure contributes to substantial increase of thermal stability up to ~400 °C.

3.3. UV/Vis spectroscopy

In the UV–Vis spectra of lanthanide complexes two main absorption bands are observed: *B* band (at 340–380 nm) and *Q* band (at 670–700 nm). As it was shown earlier for other lanthanide monophthalocyaninates [28] the lanthanide ion nature does not influence the *Q* band position (Table 2).

The presence of chlorine atoms in both α- and β-positions results in about 20 nm bathochromic shift of the *Q* band going from octa-Cl-substituted compounds to hexadeca-Cl-substituted analogs (Fig. 4), which can be explained by the weak resonance donor (+M) effect of chlorine groups. According to literature [31], the introduction of electron-donating substituents to four α-positions of the phthalocyanine macrocycle results in a bathochromic shift of the *Q* band.

In the UV–Vis spectrum of double-decker complex **5** (Fig. 4B), splitting of the *Q* band was observed with the corresponding maxima at 637 and 682 nm. This can be explained by the following. In the reduced state of general formula $[(Pc^{2-})_2Ln^{3+}]^-$, the SOMO orbital of the former neutral radical form of general formula $[Pc^{2-}Ln^{3+}Pc^{-}\cdot]^0$ becomes HOMO, giving rise to the HOMO → LUMO single-electron transition, which mainly contributes to the Q_2 component of the *Q* band, while the Q_1 band remains predominantly induced by the $2b_1 \rightarrow 6e_3$ single-electron transition [19].

In one-electron reduced form $[Ln^{3+}(^{Cl8}Pc^{2-})_2]^-$, the HOMO-LUMO

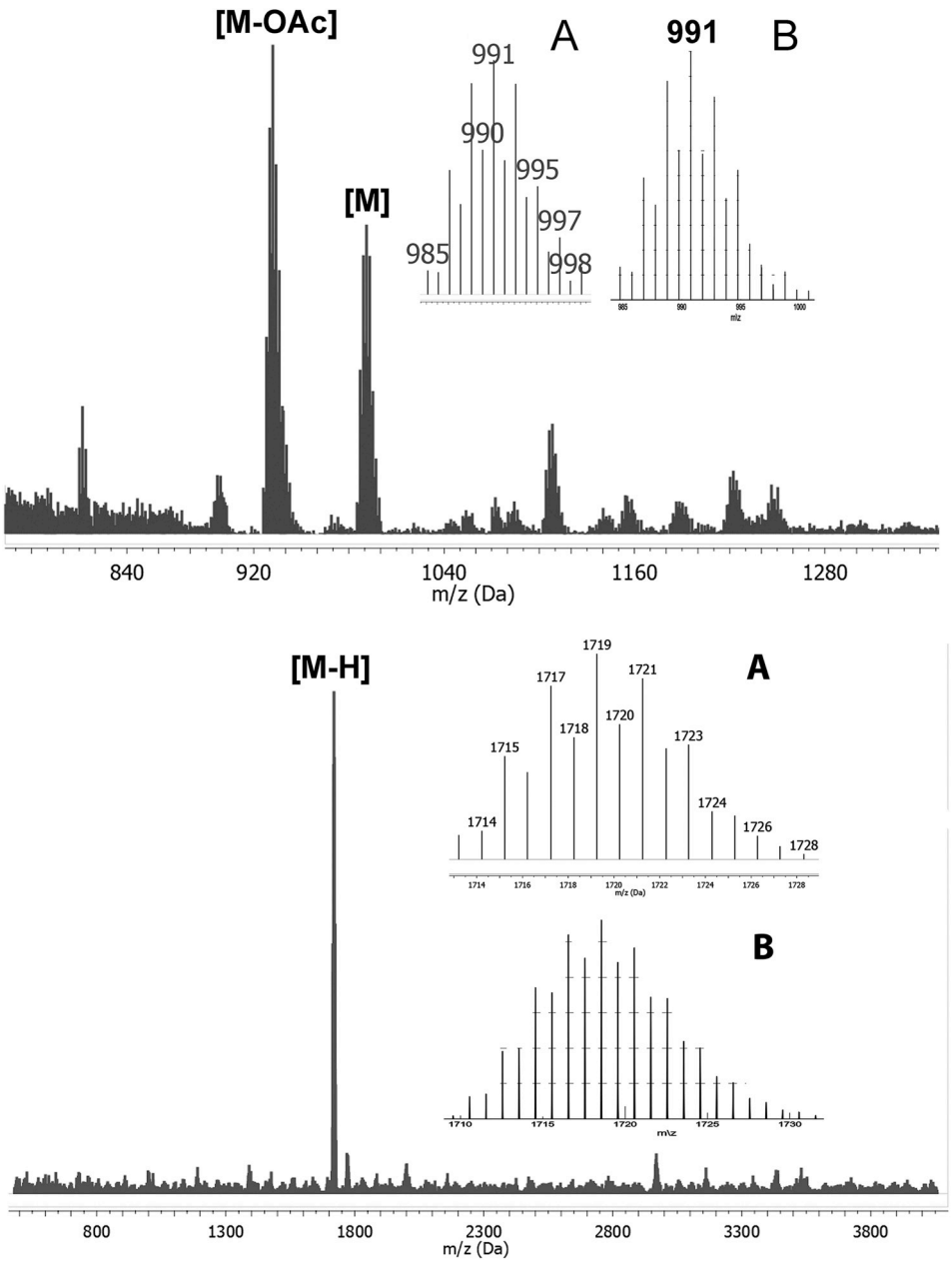

Fig. 1. MALDI-TOF mass spectra of neodymium complex **4a** in the positive ion mode (top) and **5** in the negative ion mode (bottom), obtained (inset A) and simulated (inset B) isotopic patterns of molecular ions.

gap correlates with the position of the lowest energy optical transition (Q_2) [32]. Decrease in π-π stacking interaction results in hypsochromic shift of the Q_2 band. In comparison with the anionic form of phthalimide-substituted terbium *bis*phthalocyaninate [4], a hypsochromic shift of the Q_2 band and a decrease in a distance between Q_1 and Q_2 is observed. This can be explained by destabilization of HOMO orbital due to the decrease in ionic radius going from Nd^{3+} to Tb^{3+}.

3.4. Nonlinear optical properties

The nonlinear optical studies of compounds **3**, **4** and **5** were conducted in THF and DMF using an open-aperture Z-scan technique. The obtained dependences of transmittance on the sample position are shown in Fig. 5.

Optical limiting behavior of phthalocyanine complexes can be explained by the mechanism of nonlinear absorption. If this absorption is positive, then the reverse saturable absorption (RSA) behavior takes place. The RSA occurs when the excited state absorption cross-section exceeds that of the ground state. The synthesized monophthalocyaninates **3** and **4** meet this condition (Table 3). The induced absorption due to the RSA was observed with some asymmetry of the dependencies relatively to the focal plane (Fig. 5, Fig. S7). In our case, the nonlinear absorption is determined by dynamics of the triplet state resulting from the *Q* band pumping [33,34].

To process measurement results, we used analytical model [35] taking into account the connection between amplitude and phase Gaussian beam changes that lead to the plot asymmetry. According to this model, nonlinear absorption in a far field is determined by expression:

$$T(z) = e^{-\alpha_0 L}\left(1 + T_k(z) + T_s(z) + T_c(z)\right) \quad (1)$$

where

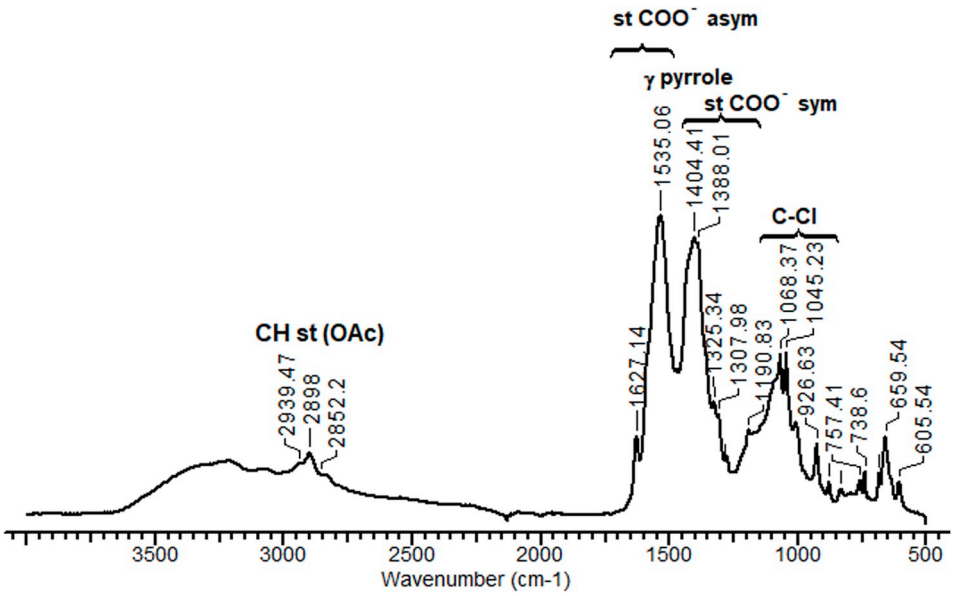

Fig. 2. IR spectra of complex **3a** on the working surface of the internal reflection (ATR) diamond element.

Table 1
^{1}H NMR data for complexes **3a**, **4a** and **5** compared to various substituted lanthanide (III) phthalocyaninates.

Compound	H_{Pc}	Ln	Solvent	Reference
3a	2.04	Pr	THF-d_8	Present paper
4a	4.74	Nd	THF-d_8	Present paper
5	5.88	Nd	THF-d_8	Present paper
^{crown}**PcNd × OAc × DBU**	4.30	Nd	$CDCl_3$	[29]
[^{crown}**Pc$_2$Nd**]$^-$	4.96	Nd	$CDCl_3$	[29]
^{Cl8}**PcEuOAc**	11.19	Eu	THF-d_8	[28]
^{Cl8}**PcErOAc**	38.21	Er	THF-d_8	[28]
^{Cl8}**PcLuOAc**	9.54	Lu	THF-d_8	[28]

$$T_k(z) = 1 + \frac{4\Delta\phi_0 x}{(x^2+1)((x^2+9)} + \frac{4\Delta\phi_0^2 x)(3x^2-5)}{(x^2+1)(x^2+9)(x^2+25)} \quad (2)$$

$$T_s(z) = \frac{8\Delta\phi_0 S x}{(x^2+1)^2(x^2+25)} - 2\Delta\phi_0 S\left[\frac{(x^2+15)}{(x^2+1)^2(x^2+9)(x^2+25)} - \frac{(x^2+7)}{(x^2+1)^3(x^2+49)}\right] \quad (3)$$

$$T_c(z) = \frac{\Delta\psi_0(x^2+3)}{(x^2+1)(x^2+9)} + \frac{12\Delta\psi_0\Delta\phi_0 x}{(x^2+1)^2(x^2+25)} + \frac{5\Delta\psi_0\Delta\phi_0 x}{2}\left[\frac{(x^2+15)}{(x^2+1)^2(x^2+9)(x^2+25)} - \frac{(x^2+7)}{(x^2+1)^3(x^2+49)}\right] \quad (4)$$

where $\Delta\psi_0 = \alpha_0 L_{eff} S$, $T_k(z)$ – open aperture transmission, $T_s(z)$ correction due saturation, $T_c(z)$ – includes effect of interaction absorption and refraction nonlinearities, $x = z/z_0$ – normalized sample position, σ_0 and σ_1 – the absorption cross section of ground state and first triplet state, respectively.

For the effective implementation of the RSA mechanism, high values of σ_1 and σ_1/σ_0 should be observed.

The data collected in Table 3 allow one to trace three main patterns.

Firstly, Nd(III) single-deckers **4** reveal increased σ_1/σ_0 values compared to Pr(III) relatives **3**. This fact correlates well with the data published for both single- and double-decker Nd(III) phthalocyanines [38–40] and their Pr(III) analogs [41]. Since structural and physicochemical characteristics of Pr(III) and Nd(III) phthalocyaninates are very close, we associate this difference in σ_1/σ_0 ratios with the different intrinsic electronic structure of these two lanthanide (III) ions. Indeed, they possess different ground state absorption, emission and excited state absorption spectra [42–47]. It is also noteworthy that Nd(III) ion has a more intense absorption near 532 nm (radiation emitted by the Nd:YAG laser used in this work) and at higher wavelengths than Pr(III).

Secondly, an increase in σ_1/σ_0 values was observed with an increase in the number of chlorine atoms in the phthalocyanine ligand from 8 (compounds **a**) to 16 (compounds **b**). This regularity can be explained by the redistribution of electron density both in the ground and in the excited states, which is associated with an increase in the electronic deficiency of the phthalocyanine decks in compounds **b** compared to **a**.

Owing to these two peculiarities, compound **4b** shows highest σ_1 and σ_1/σ_0 values across the complexes studied herein.

Thirdly, single-deckers **3** and **4** show better responses than double-decker sandwich **5**. This may be due to a cumulative effect of a lower molecular symmetry of **3** and **4** and stronger influence of the acceptor chlorine substituents to their hyperpolarizability compared to **5**. It also should be noted that, according to literature sources [38–40], Nd(III) single-decker and double-decker sandwich phthalocyaninates generally show comparable third-order nonlinear optical characteristics. The literature data [40] also correspond well to the results obtained in the current work for compound **5**.

The first triplet state (σ_1) value for **4b** is one order higher, than corresponding ones for halogen-substituted complexes with the elements of the middle and beginning of lanthanide row, which were earlier described [20]. The values of σ_1 and σ_1/σ_0 for **4b** are higher than those for the amino-substituted zinc phthalocyanine [37] and 2, 3-octa-(2-ethyl-hexyloxy)phthalocyaninato indium complex [36]. The higher σ_1/σ_0 value of ethylthiophenyl-substituted lutetium complex (^{EtPh8}**PcLuOAc)** [18] is probably due to its better solubility compared to **4b** (Table 3).

During the aging of the solutions (1–2 months) the decrease in nonlinear responses was observed due to the demetallation of target complexes and corresponding lose of solubility (UV–Vis control). It can be explained by large ionic radii of central lanthanide ions.

4. Conclusions

Novel single-decker octa- and hexadeca-Cl-substituted Pr(III) and Nd(III) phthalocyaninates were obtained in high yields (up to 76%) using multi-step approach through the formation of corresponding

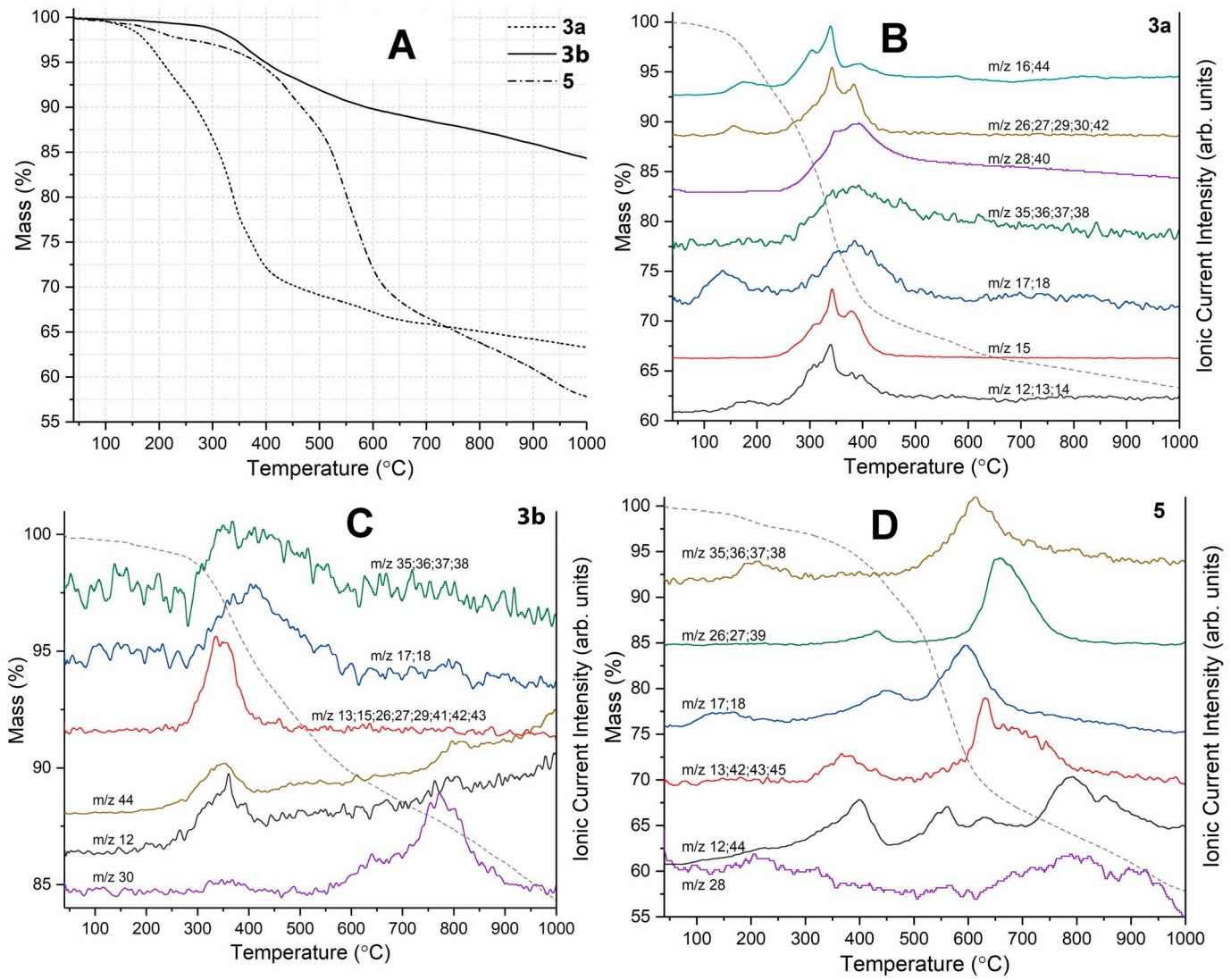

Fig. 3. Thermograms of octachloro- (**3a**, dashed line) and hexadecachloro-substituted (**3b**, solid line) praseodymium (III) phthalocyaninate and neodymium (III) *bis*phthalocyanine complex (**5**, dash-dotted line) (A). Evolved gas analysis-mass spectrometry for corresponding compounds (B–D).

Table 2
UV–Vis data in THF.

Compound	*B* band	*Q* band	Reference
3a	346	672	Present paper
3b	379	693	Present paper
4a	349	673	Present paper
4b	378	694	Present paper
5	340	637 and 682	Present paper
^{Cl8}**PcEuOAc**	346	677	[28]
^{Cl8}**PcErOAc**	349	676	[28]
^{Cl8}**PcLuOAc**	349	676	[28]
^{Cl16}**PcEuOAc**	378	696	[16]
^{Cl16}**PcErOAc**	361	696	[16]
^{Cl16}**PcLuOAc**	363	699	[16]

phthalocyanine ligand. Direct synthesis of sandwich-type chloro-substituted Nd(III) *bis*phthalocyaninate was carried out using two pre-formed synthetic blocks: octachloro-substituted phthalocyanine ligand and neodymium (III) monophthalocyaninate. Neodymium (III) *bis*phthalocyaninate is formed in redox stable anionic form $[(^{Cl8}Pc^{2-})_2Nd^{3+}]^-$. Storage of its THF solution in air for several days does not affect the spectrum line shape: the characteristic π-radical band at 400–500 nm does not appear. It results from electron-withdrawing effect of peripheral chlorine groups. The presence of Pr(III) or Nd(III) central ions results in an upfield shift of the aromatic proton signals in the ^{1}H NMR spectra of target complexes comparing to the corresponding octachloro-substituted diamagnetic lutetium (III) phthalocyaninates. The strongest upfield shift of the aromatic proton signals (2.04 ppm) was observed for octachloro-substituted Pr(III) complex. In contrast to lanthanide (III) *bis*phthalocyaninates, bearing electron-releasing functional groups, NMR spectrum of chloro-substituted neodymium (III) *bis*phthalocyaninate was measured without addition of any reducing agents. Thermogravimetry revealed greater thermal stability of perchloro-substituted Pr(III) phthalocyaninate and double-decker complex (up to 400 °C) in comparison with octachloro-substitued praseodymium phthalocyaninate. The presence of chlorine atoms in a both α-and β-positions results in about 20 nm bathochromic shift of the *Q* band going from octachloro-substituted compounds to hexadecachloro-substituted analogs. All chloro-substituted lanthanide (III) monophthalocyaninates demonstrate RSA effect. The highest absorption cross section of the first triplet state value ($\sigma_1 = 11.1 \times 10^{-16}$ cm^{-2}) was observed for hexadecachloro-substituted Nd(III) complex.

Declaration of competing interests

The authors declare that they have no known competing financial

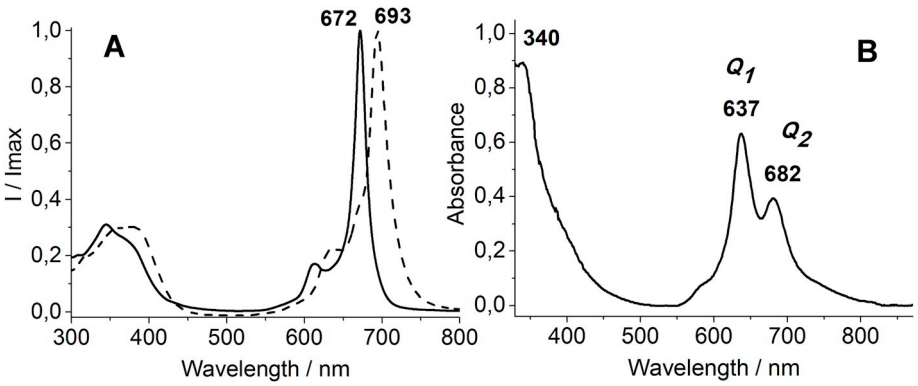

Fig. 4. UV–Vis spectra of octa-Cl- **3a** (solid line) and hexadeca-Cl-substituted **3b** (dashed line) Pr(III) phthalocyaninate in THF (A). UV–Vis spectrum of sandwich-type complex **5** (B).

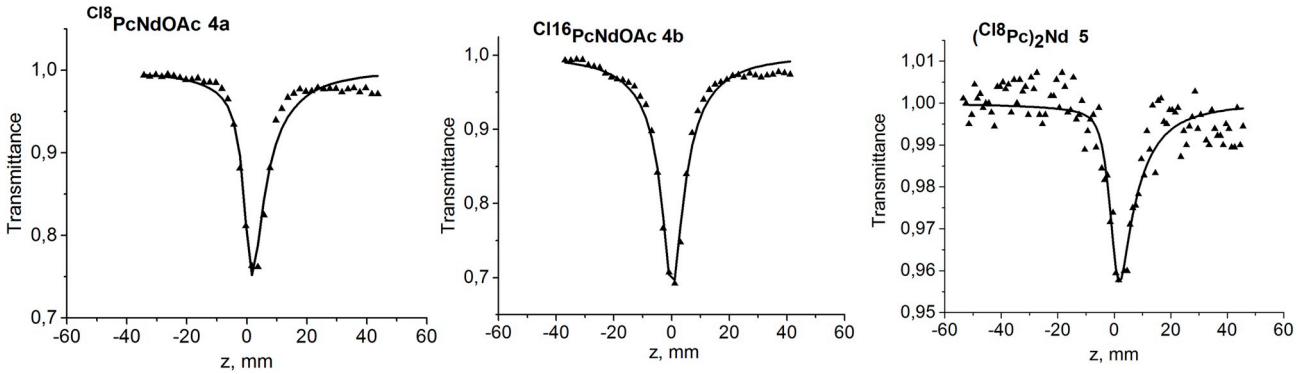

Fig. 5. Z-scan results (dotted lines) and model approximation (solid lines) for Nd(III) phthalocyaninates **^{Cl8}PcNdOAc**, **^{Cl16}PcNdOAc** and **(^{Cl8}Pc)$_2$Nd** in THF.

Table 3
NLO data.

Compound (Solvent)	Initial transmittance	Concentration, M	$\sigma_1 \times 10^{-16}$ cm^2	$\sigma_0 \times 10^{-18}$ cm^2	σ_1/σ_0	Reference
^{Cl8}PcPrOAc, 3a (THF)	0.82	10^{-4}	1.5	1.96	76.5	Present paper
^{Cl8}PcPrOAc, 3a (DMF)	0.81	10^{-4}	2.1	1.96	107.1	Present paper
^{Cl16}PcPrOAc, 3b (THF)	0.71	2.3×10^{-4}	1.4	1.19	117.6	Present paper
^{Cl16}PcPrOAc, 3b (DMF)	0.69	10^{-4}	0.9	1.19	75.6	Present paper
^{Cl8}PcNdOAc, 4a (THF)	0.83	2.2×10^{-4}	8.1	2.8	289.3	Present paper
^{Cl16}PcNdOAc, 4b (THF)	0.79	2.2×10^{-4}	**11.1**	2.3	**482.6**	Present paper
(^{Cl8}Pc)$_2$Nd, 5 (THF)	0.63	10^{-4}	1.5	3.3	45.5	Present paper
(^{Cl8}Pc)$_2$Nd, 5 (DMF)	0.62	10^{-4}	2.1	2.6	80.8	Present paper
$^{EHO}{}_8$PcIn(OCOCF$_3$)	not presented	not presented	1.3	22	5.9	[36]
ZnPc-NH$_2$ (DMSO)	not presented	not presented	0.0635	0.133	48	[37]
($^{t\text{-}Bu}$Pc)$_2$Eu (THF)	not presented	5×10^{-5}	2.2	47	4.7	[10]
^{Cl16}PcTbOAc (THF)	not presented	not presented	1.96	8.6	22.8	[20]
^{Cl16}PcEuOAc (THF)	not presented	not presented	0.96	10.7	10.3	[20]
^{Cl16}PcLuOAc (THF)	not presented	not presented	0.76	16.0	4.8	[20]
^{EtPh8}PcLuOAc (THF)	not presented	10^{-3}	7.3	1.3	**561**	[18]

interests or personal relationships that could have appeared to influence the work reported in this paper

CRediT authorship contribution statement

Elena A. Kuzmina: Methodology, Validation, Investigation, Writing - original draft. **Tatiana V. Dubinina:** Conceptualization, Writing - original draft, Formal analysis, Funding acquisition. **Nataliya E. Borisova:** Writing - review & editing, Visualization, Investigation. **Boris N. Tarasevich:** Writing - review & editing, Investigation. **Vitaly I. Krasovskii:** Software, Writing - review & editing. **Ivan N. Feofanov:** Investigation, Data curation. **Alexander V. Dzuban:** Investigation, Data curation. **Larisa G. Tomilova:** Supervision, Writing - review & editing, Project administration, Funding acquisition.

Acknowledgements

We are grateful to the Russian Science Foundation (Grant 17-13-01197) for main support of this research. Development of synthetic approaches to halogen-substituted complexes was supported by the Council under the President of the Russian Federation for State Support of Young Scientists and Leading Scientific Schools (Grants MK-3115.2018.3). Investigation of NLO properties was performed within the Basic research program of RAS “Photonic technologies in sensing of inhomogeneous media and biological objects”.

Appendix A. Supplementary data

Supplementary data to this article can be found online at https://doi.org/10.1016/j.dyepig.2019.108075.

References

[1] Kim K, Kwak TH, Cho MY, Lee JW, Joo J. Synth Met 2008;158:553–5.
[2] Yang RD, Park J, Colesniuc CN, Schuller IK, Royer JE, Trogler WC, Kummel AC. J Chem Phys 2009;130:164703.
[3] Schlettwein D, Woehrle D, Karmann E, Melville U. Chem Mater 1994;6:3–6.
[4] Gonidec M, Amabilino DB, Veciana J. Dalton Trans 2012;41:13632–9.
[5] Lu G, Bai M, Li R, Zhang X, Ma C, Lo P-C, Ng DKP, Jiang J. Eur J Inorg Chem 2006; 2006:3703–9.
[6] de la Torre G, Vázquez P, Agulló-López F, Torres T. Chem Rev 2004;104:3723–50.
[7] Miao Q, Sun E, Liang M, Liu Q, Xu Y. Comput. Theor. Chem. 2017;1104:32–6.
[8] Oluwole DO, Yagodin AV, Britton J, Martynov AG, Gorbunova YG, Tsivadze AY, Nyokong T. Dalton Trans 2017;46:16190–8.
[9] Dini D, Calvete MJF, Hanack M. Chem Rev 2016;116:13043–233.
[10] Karpo AB, Pushkarev VE, Krasovskii VI, Tomilova LG. Chem Phys Lett 2012;554: 155–8.
[11] Kuzmina EA, Dubinina TV, Tomilova LG. New J Chem 2019;43:9314–27.
[12] Dini D, Yang GY, Hanack M. J Chem Phys 2003;119:4857–64.
[13] Oluwole DO, Ngxeke SM, Britton J, Nyokong T. J Photochem Photobiol A Chem 2017;347:146–59.
[14] Wang H, Wang B-W, Bian Y, Gao S, Jiang J. Coord Chem Rev 2016;306:195–216.
[15] Bertani F, Cristiani N, Mannini M, Pinalli R, Sessoli R, Dalcanale E. Eur J Org Chem 2015;2015:7036–42.
[16] Kuzmina EA, Dubinina TV, Zasedatelev AV, Baranikov AV, Makedonskaya MI, Egorova TB, Tomilova LG. Polyhedron 2017;135:41–8.
[17] Sheik-Bahae M, Said AA, Wei TH, Hagan DJ, Stryland EWV. IEEE J Quantum Electron 1990;26:760–9.
[18] Dubinina TV, Tychinsky PI, Borisova NE, Krasovskii VI, Ivanov AS, Savilov SV, Maklakov SS, Sedova MV, Tomilova LG. Dyes Pigments 2018;156:386–94.
[19] Pushkarev VE, Tomilova LG, Nemykin VN. Coord Chem Rev 2016;319:110–79.
[20] Kuzmina EA, Dubinina TV, Dzuban AV, Krasovskii VI, Maloshitskaya OA, Tomilova LG. Polyhedron 2018;156:14–8.
[21] Mørkved EH, Afseth NK, Kjøsen H. J Porphyr Phthalocyanines 2006;10:1301–8.
[22] Gorbunova YG, Lapkina LA, Martynov AG, Biryukova IV, Tsivadze AY. Russ J Coord Chem 2004;30:245–51.
[23] Dubinina TV, Paramonova KV, Trashin SA, Borisova NE, Tomilova LG, Zefirov NS. Dalton Trans 2014;43:2799–809.
[24] Dubinina TV, Kosov AD, Petrusevich EF, Maklakov SS, Borisova NE, Tomilova LG, Zefirov NS. Dalton Trans 2015;44:7973–81.
[25] Pushkarev VE, Shulishov EV, Tomilov YV, Tomilova LG. Tetrahedron Lett 2007;48: 5269–73.
[26] Nakamoto K. Infrared and Raman spectra of Inorganic and coordination compounds. A Wiley-Interscience Publication John Wiley and Sons; 1986.
[27] Kosov AD, Dubinina TV, Borisova NE, Ivanov AV, Drozdov KA, Trashin SA, De Wael K, Kotova MS, Tomilova LG. New J Chem 2019;43:3153–61.
[28] Kuzmina EA, Dubinina TV, Borisova NE, Tomilova LG. Macroheterocycles 2017;10: 520–5.
[29] Nefedova IV, Gorbunova YG, Sakharov SG, Tsivadze AY. Russ J Inorg Chem 2005; 50:165–73.
[30] Li X, Qi D, Chen C, Yang L, Sun J, Wang H, Li X, Bian Y. Dyes Pigments 2014;101: 179–85.
[31] Kobayashi N, Ogata H, Nonaka N, Luk'yanets EA. Chem Eur J 2003;9:5123–34.
[32] Wang R, Li R, Bian Y, Choi C-F, Ng DKP, Dou J, Wang D, Zhu P, Ma C, Hartnell RD, Arnold DP, Jiang J. Chem Eur J 2005;11:7351–7.
[33] Zasedatelev A, Karpo A, Feofanov I, Krasovskii V, Pushkarev V. J Phys Conf Ser 2014;541:012064.
[34] Tutt LW, Boggess TF. Prog Quantum Electron 1993;17:299–338.
[35] Wang Y, Saffman M. Opt Commun 2004;241:513–20.
[36] Dini D, Calvete MJF, Hanack M, Chen W, Ji W. ARKIVOC 2006:77–96.
[37] Bankole OM, Nyokong T. J Photochem Photobiol A Chem 2016;319–320:8–17.
[38] Sekhosana KE, Amuhaya E, Nyokong T. Polyhedron 2016;105:159–69.
[39] Sekhosana KE, Shumba M, Nyokong T. Polyhedron 2017;138:154–60.
[40] Sekhosana KE, Nkhahle R, Nyokong T. Chemistry 2018;3:6671–82.
[41] Ren B, Sheng N, Gu B, Wan Y, Rui G, Lv C, Cui Y. Dyes Pigments 2017;139:788–94.
[42] Kück S, Fornasiero L, Mix E, Huber G. Appl Phys B 1998;67:151–6.
[43] De Camargo ASS, Silva RA, Andreeta JP, Nunes LAO. Appl Phys B 2005;80: 497–502.
[44] Soulard R, Xu B, Doualan JL, Camy P, Moncorgé R. J Lumin 2012;132:2521–4.
[45] Okamoto H, Kasuga K, Hara I, Kubota Y. Opt Express 2009;17:20227–32.
[46] Gorieva V, Korableva S, Semashko V. Opt Mater Express 2016;6:1146–50.
[47] Schroll CA, Lines AM, Heineman WR, Bryan SA. Anal. Methods. 2016;8:7731–8.